Vision enhancement for maritime search and rescue operations at night and bad weather conditions

Tristan Preis[1], Jendrik Schmidt[1], Alexander Klein[1], Enno Peters[1], Thomas Lübcke[2], and Maurice Stephan[1]

[1]German Aerospace Center (DLR) Institute for the Protection of Maritime Infrastructures, Bremerhaven, Germany.
[2]German Maritime Search and Rescue Service (DGzRS), Bremen, Germany.

***Abstract*—During search and rescue operations (SAR) at night and bad weather conditions, the detection of persons in water represents a major challenge. When conventional searchlights are used, the backscattering from rain and fog decreases the detection range. For these conditions, the transportable range-gated viewing system (TRAGVIS) was developed, aiming to reduce the effect of backscatter, in particular from close ranges (up to several hundred meters). After data acquisition, image post processing techniques were applied. The objective of the study presented here is to enchance the vision of the image for better object recognition by the operator. In addition automatic object detection methods were tested.**

***Index Terms*—Vision enhancement, non-uniformity correction, NUC, image processing, gated viewing, range-gated viewing, equalization, object detection, YOLOv8.**

I. Introduction

As part of the project TRAGVIS [1] and in cooperation with the German Maritime Search and Rescue Service (Deutsche Gesellschaft zur Rettung Schiffbrüchiger, DGzRS) a range-gating instrument was developed aiming at detecting persons overboard and other floating objects during nighttime. The TRAGVIS is an active imaging sensor aiming to enhance vision in darkness and scattering environments (fog, rain, snow). A technology demonstration was performed at the German North Sea in the vicinity of Bremerhaven onboard the rescue cruiser 'Hermann Rudolf Meyer' at the 6th of December 2022 during nighttime (darkness). During the field test, a dummy without retroreflectors, a floating bouy with retroreflectors and the daughter boat were used as objects to be detected by the TRAGVIS. An example scene of the field test is shown in Figure 1. The figure shows identical scenes recorded simultaneously by the TRAGVIS, the thermal- and the optical camera (for the visible range), respectively. In the image the daughter boat and a dummy without retroreflectors can be seen (Fig 1a). The major part of the image appears to be dark.

In Figure 1b, the daughter boat can be seen in the thermal image, due to the movement of the see the dummy is not distinguishable from the surrounding waves. With the optical camera only the navigational lights are visible in Figure 1c. In comparison to the image recorded with TRAGVIS (Fig. 1a), the images shown in Figure 1b and Figure 1c provide no benefit for the search and rescue operator in terms of detecting the dummy (person overboard). This study aims at improving the TRAGVIS image further enabling an even better (and more reliable) detection of persons overboard spottet by human instrument operators.

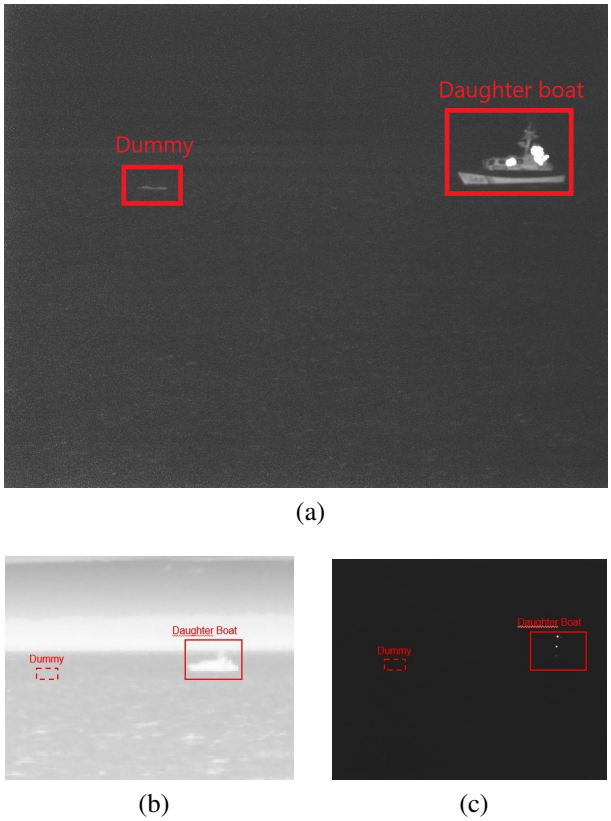

Figure 1. Scene taken with (a) TRAGVIS (original, i.e. without post-processing), (b) thermal camera and (c) optical camera

The measurement technique is explained in Section II. Briefly, the instrument provides grayscale images, which are presented as the intensity of a reflection. Darker objects in an image can be increased in brightness with post-processing techniques, described in Section III, and therefore can be detected better by manual inspection of a human operator. In addition, image quality is increased in terms of noise reduction applying a non-uniformity correction (NUC) [2]. After reducing noise by the NUC an equalization step can be done, in which the pixel values can be adjusted to provide more information in the image.

Despite vision enhancement by gated viewing and subsequent post-processing focusing at better recognition by human

operators, an automatic, computer assisted object detection was tested aiming to replace or support the human search and rescue operator. However, the object detector must be trained for these specific objects.

In Section IV the results after the processing steps are evaluated and discussed and lastly in Section V the results will be concluded and an outlook for future possible works will be given.

II. Instrument and Measurement Technique

In a first, hardware-based step, the attempt is to physically reduce backscattering from rain or fog in front of the sensor system by range-gating. The measuring technique of range-gated viewing [3] is to illuminate and record a specific depth level of a scene, as illustrated in Figure 2. A pulsed laser illuminator is synchronized with a camera, that can open and close the electronic shutter in nanoseconds. The adjustable delay between emission of the laser pulse and opening of the camera shutter allows to exclude non-essential parts of an image, which then consists of a defined 'gate', that is illuminated. Images, taken with TRAGVIS operating in the near infrared spectral region at approx. 808 nm, are grayscale images produced by the intensity reflected by an object.

Retroreflectors are usually saturated in such images and can be recognized easily. Even with a normal searchlight in the visible spectrum, objects with retroreflectors can be spotted better than without reflectors. For this reason, many life vests and other objects designed to be seen, are equipped with retroreflectors [4]. However, in some cases, persons overboard do not wear special clothing with retroreflectors, which leads to a less bright reflection in the image and makes the detection more difficult during a search and rescue operation.

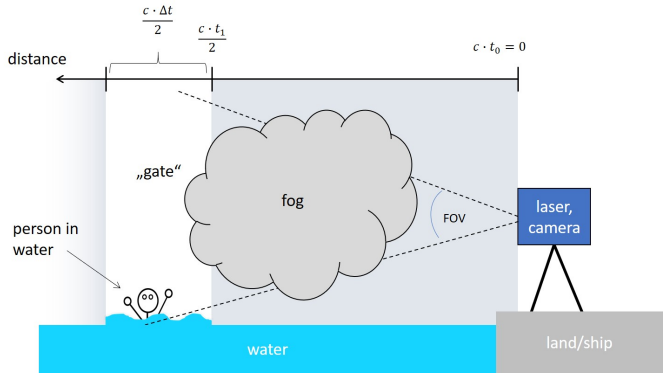

Figure 2. Measuring technique range-gated viewing.

The main objective of this project was to find people in distress at sea, therefore a wide field of view (FOV) of 7° x 6° was chosen (which is relatively large for a laser) to cover a large area in each image. The maximum detection range under fog conditions is ≈ 250 m. Eye-safety is of course of major concern. Therefore, a self-build beam expander was developed, which shapes the beam and produces the FOV. The resulting instrument fulfills the requirement of a laser class 1M system.

III. Post-processing

After acquiring an image, a non-uniformity correction (NUC) is performed. The resulting image of a 1-point NUC $\boldsymbol{x}_{1-NUC}$ is calculated, by subtracting a reference (dark) image $\boldsymbol{x}_{ref,dark}$ from the recorded image $\boldsymbol{x}_{obj}$ (eq. (1)) and corrects for the so-called dark signal non uniformity (DSNU). Therefore, a dark image is acquired with a closed shutter accounting for thermally induced dark current of each pixel of the camera (i.e. thermally generated electrons) and electronic offsets.

$$\boldsymbol{x}_{1-NUC} = \boldsymbol{x}_{obj} - \boldsymbol{x}_{ref,dark} \tag{1}$$

After the subtraction of the dark image, the average of the dark image $\overline{x_{ref,dark}}$ can be added to all pixels (eq. (2)). This results in an image $\boldsymbol{x}_{1-NUC,mean}$ having the same background gray value but better uniformity.

$$\boldsymbol{x}_{1-NUC,mean} = \boldsymbol{x}_{obj} - \boldsymbol{x}_{ref,dark} + \overline{x_{ref,dark}} \tag{2}$$

The idea of a further 2-point NUC is to reduce the spatial noise, caused by the different sensitivities of the pixels when exposed to light, which leads to the so-called Photo-Response Non-Uniformity (PRNU). Therefore, the matrix $\boldsymbol{m}$ (eq. (3)) is introduced. The matrix consists of a reference image $\boldsymbol{x}_{ref,mid}$, in which the sensor is illuminated by a homogenous light, and a reference (dark) image $\boldsymbol{x}_{ref,dark}$.

$$\boldsymbol{m} = \frac{\overline{x_{ref,mid}} - \overline{x_{ref,dark}}}{\boldsymbol{x}_{ref,mid} - \boldsymbol{x}_{ref,dark}} \tag{3}$$

After multiplying the image with $\boldsymbol{m}$, all pixel photo-respnsivities have the same slope[1]. As for the 1-point NUC, the mean of the dark image might or might not be added to the corrected image.

$$\boldsymbol{x}_{2-NUC} = (\boldsymbol{x}_{obj} - \boldsymbol{x}_{ref,dark})m \tag{4}$$

$$\boldsymbol{x}_{2-NUC,mean} = (\boldsymbol{x}_{obj} - \boldsymbol{x}_{ref,dark})\boldsymbol{m} + \overline{x_{ref,dark}} \tag{5}$$

To highlight more details, the image can be equalized. The major parts, that are recorded during night over water, are usually dark. By brightening up the scene, more details can be seen by the search and rescue operator. Therefore an equalizer algorithm is adopted, that is usally used for astrophotography[2]. The equalization process can be separated into two functions $f(x)$ and $g(x)$, which are called subsequently.

The function $f(x)$ is boosting dark grey values towards brighter values, but not pushing over the displayable limit, as shown in Figure 3. Details at the dark grey scale are more contrasted.

Function $g(x)$ pushes dark and bright pixel values to the middle of the grey value range, as illustrated in Figure 3. Brighter objects become more darker and dark objects become

[1]The 2-point NUC suggested here assumes a linear photo-response.
[2]https://yager.io/Astro.html#Post-processing

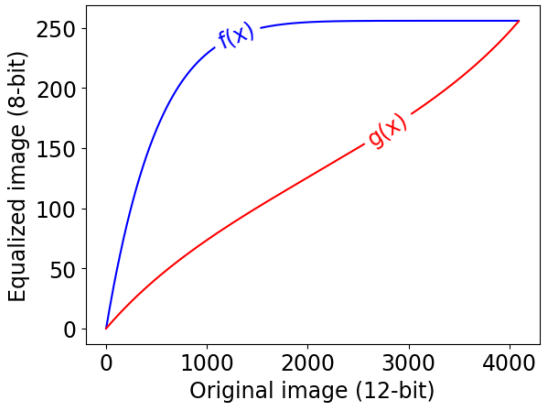

Figure 3. Equalization graphs

more brighter[3]. In these steps also the conversion from a 12-bit image to an 8-bit image is done, which leads to a tone mapping effect.

In Table I, all combinations of corrections suggested above are tested aiming at best human perception.

Table I
LIST OF PROCESSING STEPS AND RESULTING IMAGES

TRAGVIS	**Non-uniformity correction**	**Equalization**
Original		Original + EQ
	1-point NUC	1-point NUC + EQ
	2-point NUC	2-point NUC + EQ
	1-point NUC + mean	1-point NUC + mean + EQ
	2-point NUC + mean	2-point NUC + mean + EQ

For automated recognition of objects in water, the object detector YOLOv8 [5] by ultralytics is used. For training, a labeled dataset from the field test was used. The dataset was therefore extended with every intermediate post-processing step as described in Table I. By using more complex variants of the object detector, the prediction of objects in an image becomes more reliable, but the processing while training and prediction is more extensive.

IV. RESULTS

During the technology demonstration 499 different scenes were recorded with the TRAGVIS. To demonstrate the vision enchancement techniques presented in the Section II and Section III, the scene in Figure 1a is used.

In the first step a non-uniformity correction is conducted, to reduce the noise as shown in Figure 4a, Figure 4b and Figure 6[4][5]. Because of the substraction of the reference dark image $\boldsymbol{x}_{ref,dark}$, the resulting image in Figure 4a for the 1-point NUC is darker. The differentiation of the dummy in contrast to the background gets worse as the human eyes perception for darker grey intensities is poorer than for brighter grey values [6]. Therefore the average of the reference (dark) image $\overline{x_{ref,dark}}$ is added to improve the presentation for the human eye. The results are visualized for the 1-point NUC in Figure 4b.

The results after equalization are shown in Figure 4c, Figure 4d and in the Appendix in Figure 7. A significant improvement can be observed in the images of the 1-point NUC (Fig. 4c), the dummy can be spotted better in comparison to the other images before and after equalization.

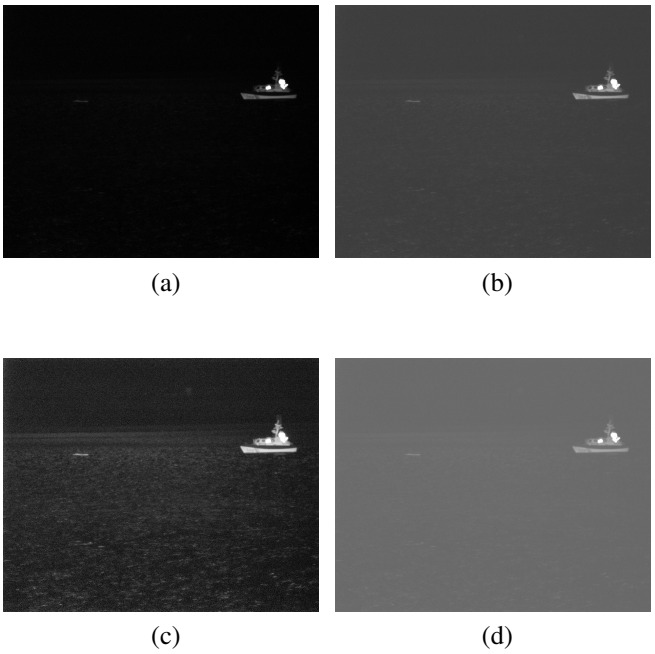

(a) (b)

(c) (d)

Figure 4. 1-point NUC (a) without and (b) with added $\overline{x_{ref,dark}}$, and after equalization (c) without and (d) with added $\overline{x_{ref,dark}}$.

To test the influence of individual processing steps on the detection of the dummy, a vertical cross section was calculated across the image when applying single processing steps, or combination of processing steps. In Figure 5 the cross section and the resulting graph of grey values along the section is shown. The dummy is pointing out with a grey value of 99 in comparison to the average of the image of 65.

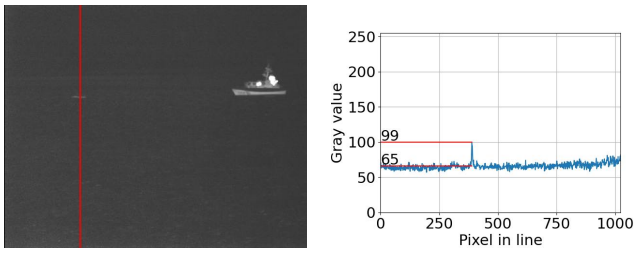

(a) (b)

Figure 5. (a) Position of vertical cross section through the image; (b) Grey values along the red line.

In order to quantitatively compare the results, the signal-to-noise ratio (SNR) and the Michelson contrast were calculated. The SNR, used for this case, was defined as the ratio of the maximum grey value of the dummy and the standard deviation of grey values in the cross section. The Michelson contrast was calculated between dummy and background value.

[3]This does not help for halos or saturation effects and blooming usually resulting from strong retro reflections.

[4]Discussed figures from Figure 6 to Figure 14 can be found in the Appendix

[5]The resulting images for the 2-point NUC can be found in the Appendix

In Table II the SNR and contrast of the dummy and the background for every processing step can be seen. The SNR in the original image is 8 and the Michelson contrast is 0.22.

Table II
SIGNAL-TO-NOISE RATIO AND MICHELSON CONTRAST FOR EVERY PROCESSING STEP

No.	Image Name	SNR	Michelson contrast
1	Original (Fig. 5a)	8	0.22
2.1	1-point NUC (Fig. 4a)	12	0.86
2.2	2-point NUC (Fig. 6a)	12	0.85
2.3	1-point NUC + mean (Fig. 4b)	12	0.23
2.4	2-point NUC + mean (Fig. 6b)	12	0.22
3.1	Original + EQ (Fig. 7a)	7	0.13
3.2	1-point NUC + EQ (Fig. 4c)	9	0.71
3.3	2-point NUC + EQ (Fig. 7b)	8	0.71
3.4	1-point NUC + mean + EQ (Fig. 4d)	11	0.12
3.5	2-point NUC + mean + EQ (Fig. 7c)	10	0.12

After the non-uniformity correction, the noise is decreased and the contrast depends on the offset of the grey values (Fig. 8). The contrast of the original image and the images after the non-uniformity correction with the added mean value is equivalent, but the SNR is increased. Without adding the average to the image the contrast for the 1-point NUC and 2-point NUC is higher, as well as the SNR. But as mentioned before, the human perception is worse at darker intensity distributions, even though the SNR and contrast are the highest values in this measurement series.

The results in Table II also display the SNR and contrast for the original and non-uniformity corrected images after equalization. The relation of the distribution among the images after equalization is nearly the same than before the equalization. The conrast is drecreased by 0.1 for every image after the equalization. The SNR is also decreased for the 1-point NUC and 2-point NUC to the value, before the correction was performed. Though the contrast and SNR are decreased, the improvement in identifing the dummy by a search and rescue operator are the best (Fig. 4c & Fig 12b).

By comparing the intensity distribution of the equalized images in Figure 9 with the resulting images in Figure 7 the contrast for the human eye is for the 1-point NUC (Fig. 9b) and 2-point NUC (Fig. 9c) the highest. Even though the noise is slightly increased by the equalization.

Results of the object detection can be found in Figures 10-14 in the Appendix and in Table III. In every image the daughter boat was deteced by 95 %. In other images typical maritime objects like boats and bouys were commonly detetced by at least 85 %.

The identification of the dummy varies from 28 % in the original (Fig. 10a) to 67 % in the 1-point NUC (Fig. 11a) image. The detection probability of the dummy for the images, that had the best contrast for identification by a human operator, is only at 51 % for 1-point NUC (Fig. 11b) and 52 % for 2-point NUC (Fig. 12b) after equalization. For other images with irregular floating objects like the dummy or a sphere with retroreflectors the detection probability varies from 0 % to 81 %.

Table III
OBJECT DETECTION: DETECTION PROBABILITY OF DUMMY

Image Name	Detection probability
Original (Fig. 10a)	28 %
Original + EQ (Fig. 10b)	31 %
1-point NUC (Fig. 11a)	67 %
1-point NUC + EQ (Fig. 11b)	51 %
2-point NUC (Fig. 12a)	60 %
2-point NUC + EQ (Fig. 12b)	52 %
1-point NUC + mean (Fig. 13a)	62 %
1-point NUC + mean + EQ (Fig. 13b)	41 %
2-point NUC + mean (Fig. 14a)	54 %
2-point NUC + mean + EQ (Fig. 14b)	53 %

By comparing the outcome of the object detection with the intensity distributions (Fig. 5b, Fig. 8 & Fig. 9) and the resulting Michelson contrast in Table II, it seems that the object detector analyzes edges and differences of the intensity distribution in an image. The influence of noise appears to have a big effect as well, especially by matching the images of the 1-point NUC before (Fig. 11a) and after (Fig. 11b) equalization and the corresponding intensity distributions (Fig. 8a & Fig. 9b). The limitation of the human eye for low pixel intensities is not a restriction for the object detector, but was not on focus here.

V. CONCLUSION

Vision enhancement techniques like TRAGVIS, non-uniformity correction and equalization improve the object detection for a search and rescue operator (Fig. 4c) and an object detector (Fig. 4a). The presented equalizer offers an advantage for the human operator, whereas the accuracy of the object detector is decreased, as low noise and high contrast images provide the highest detection probability. Also more training data is needed for the dummy and other floating objects of interest, to increase the reliability of the detected object.

For future investigations other equalizer algorithms should be investigated. Besides the introduced techniques, other mechanisms, like filtering and masking for vision enhancement should be evaluated.

ACKNOWLEDGMENTS

We acknowledge the crew of the search and rescue vessel ‘Hermann Rudolf Meyer’ from the German Maritime Search and Rescue Service (DGzRS) supporting the field test. The technical and scientific work presented here, was funded by the German Aerospace Center (DLR).

REFERENCES

[1] Peters, Enno & Schmidt, Jendrik & Jurányi, Zsófia & Berger, Marco & Scherbarth, Stefan & Lehmann, Frank. (2019). Development of a novel low-cost NIR gated-viewing sensor for maritime search and rescue applications. 3. 10.1117/12.2532538.

[2] Perry, David & Dereniak, Eustace. (1993). Linear theory of nonuniformity correction in infrared staring sensors. Optical Engineering. 32. 1854-1859. 10.1117/12.145601

[3] Laurenzis, Martin. (2012). Investigation of range-gated imaging in scattering environments. Optical Engineering. 51. 061303. 10.1117/1.OE.51.6.061303.

[4] International Maritime Organization (1989) RESOLUTION A.658(16) - Use and Fitting of Retro-Reflective Materials on Life-Saving Appliances. https://wwwcdn.imo.org/localresources/en/KnowledgeCentre/IndexofIMOResolutions/AssemblyDocuments/A.658(16).pdf
[5] https://docs.ultralytics.com/ , 16.06.2023
[6] Kimpe T, Tuytschaever T. Increasing the number of gray shades in medical display systems–how much is enough? J Digit Imaging. 2007 Dec;20(4):422-32. doi: 10.1007/s10278-006-1052-3. PMID: 17195900; PMCID: PMC3043920.
[7] Peli E. Contrast in complex images. J Opt Soc Am A. 1990 Oct;7(10):2032-40. doi: 10.1364/josaa.7.002032. PMID: 2231113.

APPENDIX
IMAGE AFTER NON-UNIFORMITY CORRECTION (NUC)

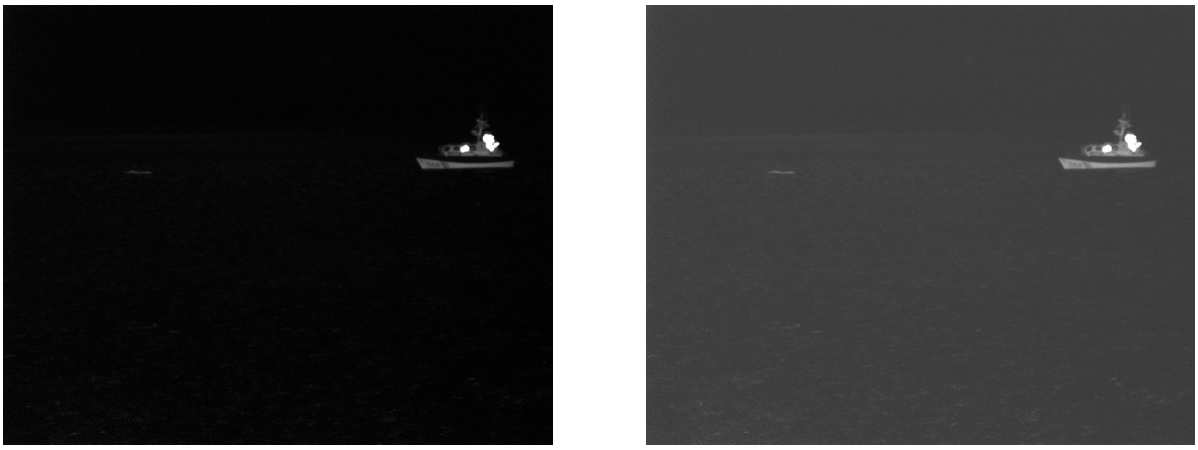

(a) 2-point NUC (b) 2-point NUC + mean

Figure 6. Example image after 2-point non-uniformity correction (NUC)

IMAGE AFTER EQUALIZATION (EQ)

(a) Original + EQ

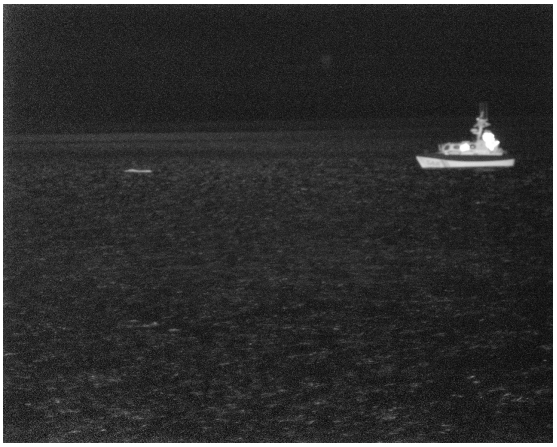

(b) 2-point NUC + EQ

(c) 2-point NUC + mean + EQ

Figure 7. Example image after equalization (EQ)

GREY VALUES ALONG THE CROSS SECTION BEFORE EQUALIZATION

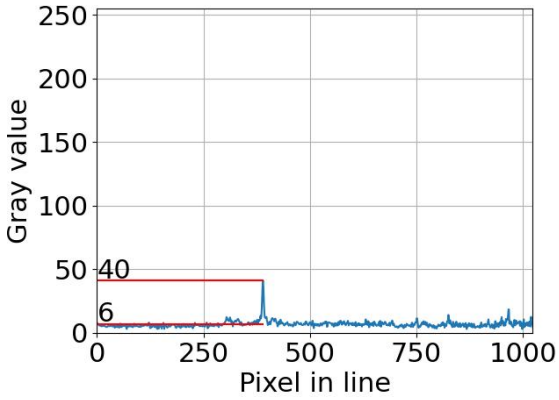

(a) Grey values: 1-point NUC (Fig. 4a)

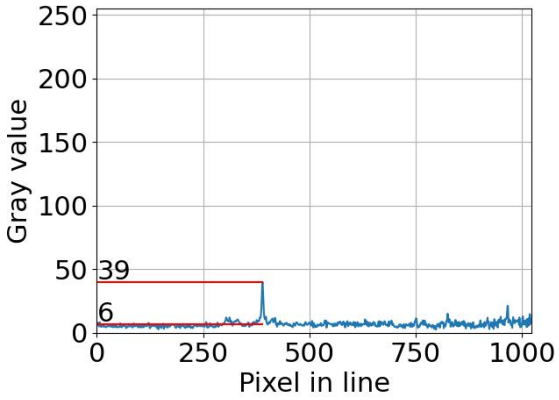

(b) Grey values: 2-point NUC (Fig. 6a)

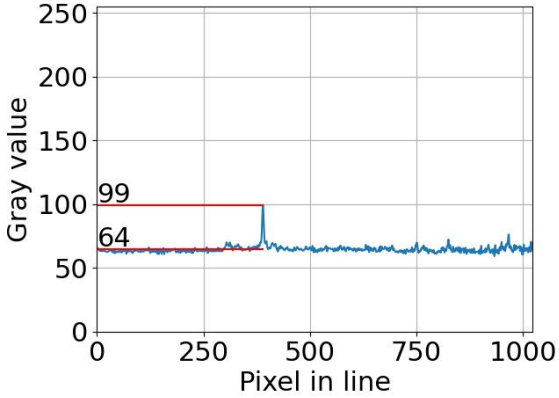

(c) Grey values: 1-point NUC + mean (Fig. 4b)

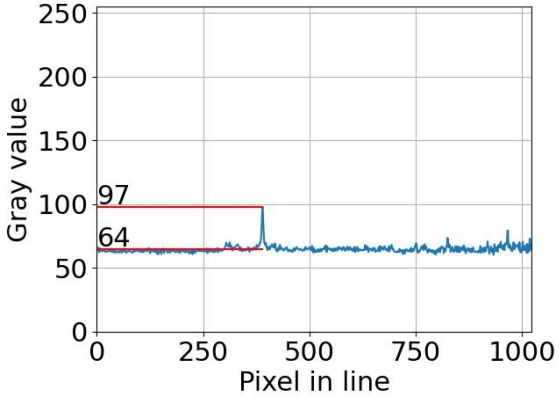

(d) Grey values: 2-point NUC + mean (Fig. 6b)

Figure 8. Graphs along the red line before equalization

GREY VALUES ALONG THE CROSS SECTION AFTER EQUALIZATION

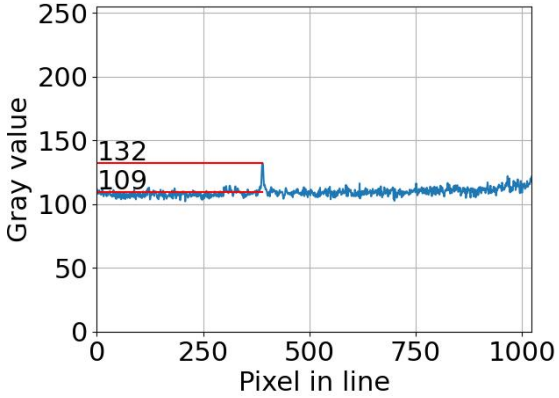

(a) Intensity distribution: Original + EQ (Fig. 7a)

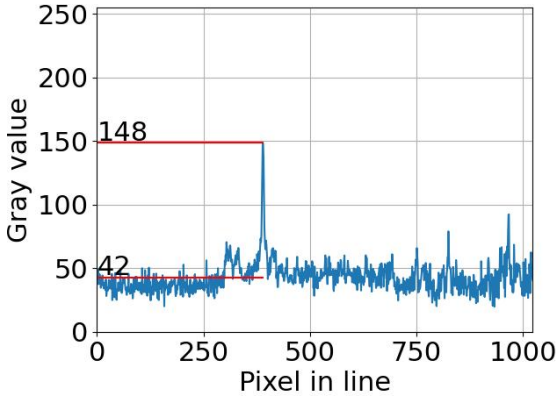

(b) Grey values: 1-point NUC + EQ (Fig. 4c)

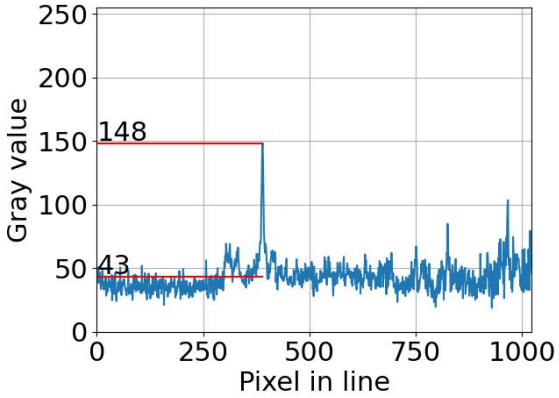

(c) Grey values: 2-point NUC + EQ (Fig. 7b)

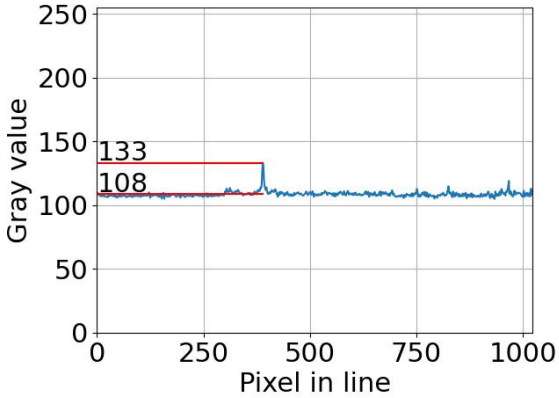

(d) Grey values: 1-point NUC + mean + EQ (Fig. 4d)

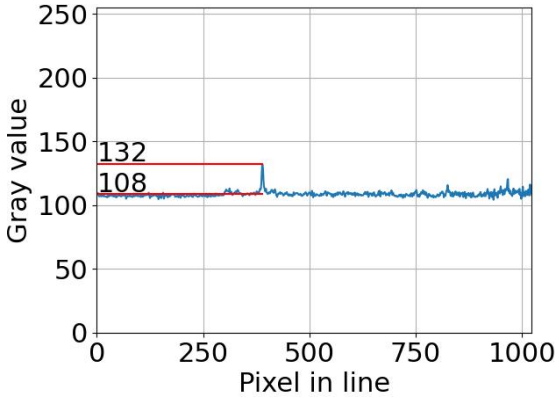

(e) Grey values: 2-point NUC + mean + EQ (Fig. 7c)

Figure 9. Graphs along the red line after Equalization (EQ)

IMAGE AFTER OBJECT DETECTION (OD)

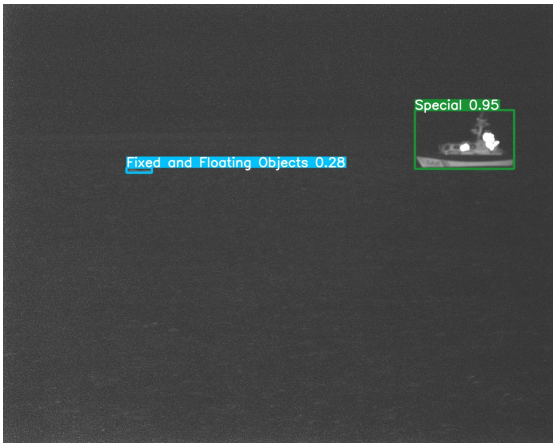

(a) OD: Original

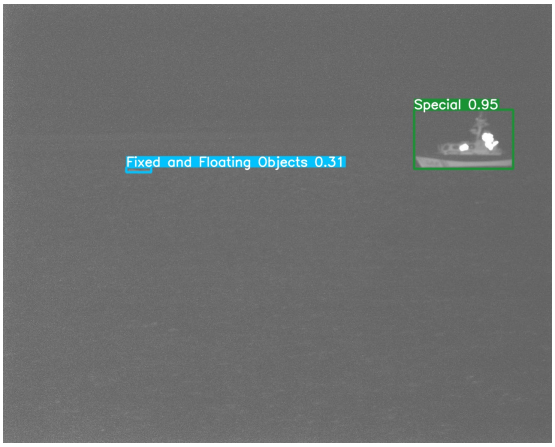

(b) OD: Original + EQ

Figure 10. Example image (original) after object detection (OD)

(a) OD: 1-point NUC

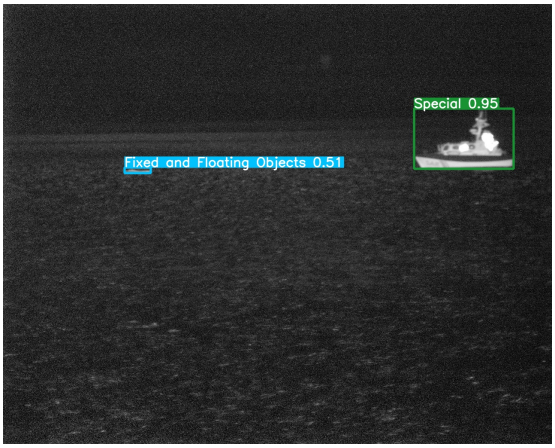

(b) OD: 1-point NUC + EQ

Figure 11. Example image (1-point NUC) after object detection (OD)

(a) OD: 2-point NUC

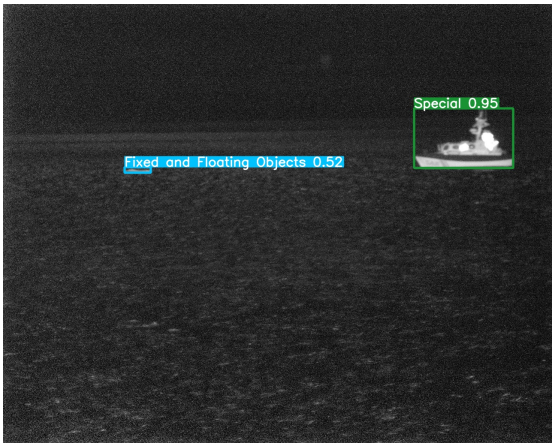

(b) OD: 2-point NUC + EQ

Figure 12. Example image (2-point NUC) after object detection (OD)

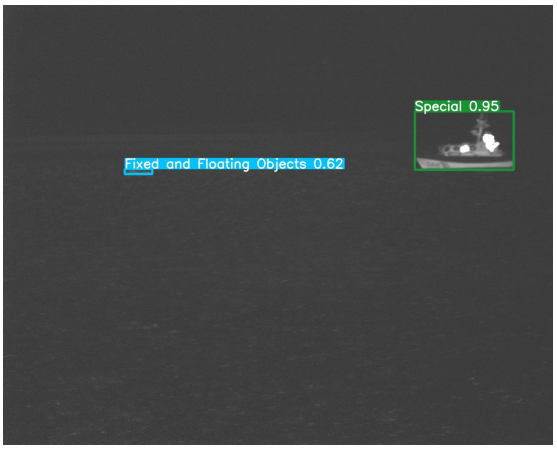

(a) OD: 1-point NUC + mean

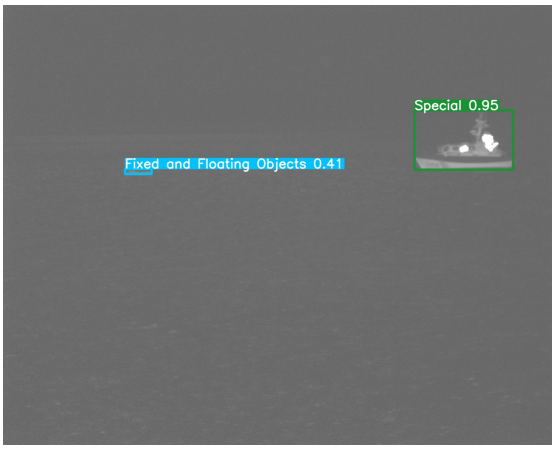

(b) OD: 1-point NUC + mean + EQ

Figure 13. Example image (1-point NUC + mean) after object detection (OD)

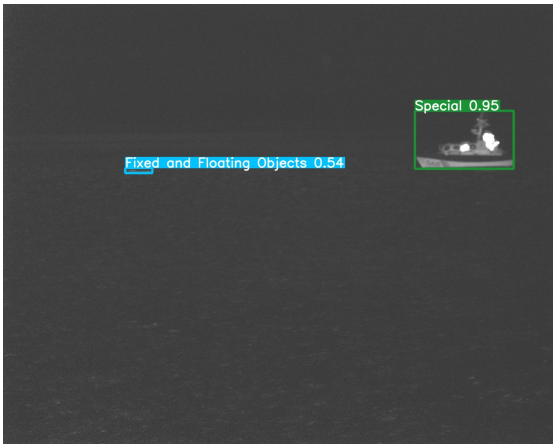

(a) OD: 2-point NUC + mean

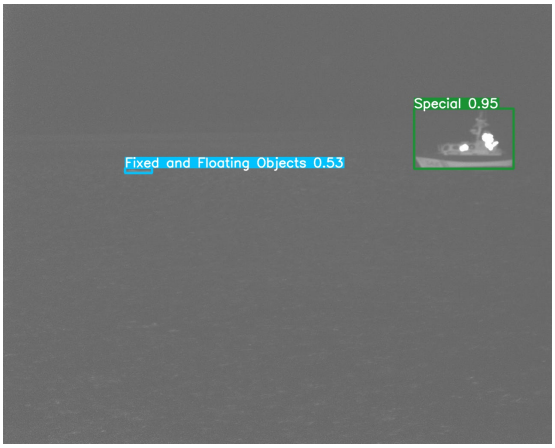

(b) OD: 2-point NUC + mean + EQ

Figure 14. Example image (2-point NUC + mean) after object detection (OD)